Iranian Journal of Medical Physics

ijmp.mums.ac.ir

Performance Evaluation of Red Light-Emitting Diodes for Therapeutic Photobiomodulation Device Design

Mohammad Reza Rashidian Vaziri[1,2], Majid Hasanabadi[3], Amirhossein Fathabadi[1,4], Mona Alikhanzadeh[1,4], Ameneh Sazgarnia[1,4*]

1. Medical Physics Research Center, Basic Sciences Research Institute, Mashhad University of Medical Sciences, Mashhad, Iran
2. Department of Physics, Faculty of Sciences, Ferdowsi University, Mashhad, Iran
3. Torbat Heydarieh University of Medical Sciences, Torbat Heydarieh, Iran
4. Department of Medical Physics, Faculty of Medicine, Mashhad University of Medical Sciences

ARTICLE INFO

Article type:
Original Paper

Article history:
Received: Aug 13, 2025
Accepted: Nov 04, 2025

Keywords:
Light Emitting Diode
Low-Level Light Therapy
Semiconductors
Spectrophotometry
Radiometry

ABSTRACT

Introduction: Photobiomodulation (PBM) therapy relies on precise control of optical parameters such as wavelength, irradiance, and beam geometry to achieve therapeutic efficacy. Light-emitting diodes (LEDs) are increasingly used in PBM devices due to their efficiency, cost-effectiveness, and spectral flexibility, but their performance varies widely with device class, drive conditions, and optical configuration. This study aimed to experimentally characterize and compare the electro-optical, thermal, and spectral properties of two commercially available classes of red LEDs—High Bright and Power—and to evaluate the effect of beam-shaping optics on achieving PBM-relevant irradiance at a clinically relevant distance.

Material and Methods: Ten units of each LED class were tested under controlled laboratory conditions. Measurements included forward voltage–current characteristics, irradiance at 10 cm, thermal rise over time, and emission spectra (peak wavelength, full width at half maximum). The effect of integrating a 30° collimating lens with the Power LED was quantified in terms of irradiance gain.

Results: At 10 cm, the High Bright LED produced sub-therapeutic irradiance (<1 mW/cm²), whereas the Power LED achieved up to 0.72 mW/cm² without optics. The Power LED exhibited a narrower spectral bandwidth (16 nm) and higher radiant output but also a greater thermal rise (~28.6 °C in 180 s). Adding the collimating lens increased irradiance by more than thirteen-fold across all voltages, enabling the Power LED to reach 10.64 mW/cm² at 2.3 V—within the PBM therapeutic range (10–50 mW/cm²). Unlike prior LED characterization studies that have primarily reported basic electro-optical parameters, this work uniquely integrates irradiance, thermal stability, and spectral analysis under clinically relevant conditions and demonstrates that a single red Power LED combined with beam-shaping optics can reliably achieve PBM-therapeutic irradiance at a practical treatment distance.

Conclusion: Power LEDs, when combined with appropriate beam-shaping optics, can deliver PBM-relevant irradiance at practical treatment distances using a single emitter. The methodology and findings are applicable to comparable AlGaInP red LEDs from multiple manufacturers and provide a framework for optimizing PBM device design across varying treatment distances and optical configurations.

► *Please cite this article as:*
Rashidian Vaziri MR, Hasanabadi M, Fathabadi A, Alikhanzadeh M, Sazgarnia A. Performance Evaluation of Red Light-Emitting Diodes for Therapeutic Photobiomodulation Device Design. Iran J Med Phys 2025; 22 (5): 341-349. 10.22038/ijmp.2025.91955.2632.

Introduction

Photobiomodulation (PBM) is a non-invasive therapeutic approach that uses low-level light in the visible to near-infrared spectrum to stimulate cellular processes, promote tissue repair, and modulate inflammation [1-3]. The therapeutic effects are primarily mediated by the absorption of photons by intracellular chromophores such as cytochrome-c oxidase, leading to enhanced mitochondrial respiration and modulation of reactive oxygen species [4, 5]. Among the various spectral regions, red light (~620–680 nm) is widely used due to its favorable balance between tissue penetration depth and chromophore absorption efficiency [6, 7].

LEDs have emerged as attractive alternatives to lasers for PBM because they are compact, energy-efficient, cost-effective, and capable of emitting at specific wavelengths with relatively narrow spectral bandwidths [8-10]. However, the therapeutic efficacy of LED-based PBM devices depends critically on several optical and electrical parameters, including peak wavelength, spectral width (full width at half maximum, FWHM), irradiance at the treatment plane, and temporal stability of output [11, 12]. One of the main challenges in LED-based PBM is achieving the required irradiance (typically 10–50 mW/cm² at the target tissue) at clinically relevant distances [13, 14]. Beam divergence inherent to LED emitters causes irradiance to decrease rapidly with distance, and thermal effects at higher drive currents can lead to output instability and spectral shifts [15, 16].

*Corresponding Author: Tel: +98-5138002316; Fax: +98-5138002320; Email: SazgarniaA@mums.ac.ir

While different types of LEDs, such as High Bright and Power LEDs, are commercially available for red-light applications, there is limited comparative data on their electro-optical performance, thermal behavior, and spectral characteristics under operating conditions relevant to PBM. Moreover, although optical beam-shaping elements such as collimating lenses are known to improve irradiance delivery, systematic experimental evaluation of their impact on achieving PBM-relevant irradiance at fixed treatment distances is scarce [17]. This gap in the literature makes it difficult for device designers to select optimal LED types and optical configurations for specific therapeutic applications. The importance of rigorous methodological evaluation in biomedical research is well recognized across diverse domains, from molecular diagnostics to therapeutic device development. Recent studies highlight how systematic characterization of tools and technologies can directly influence translational outcomes [18-22]. To date, most published studies have either focused on basic electro-optical characterization of LEDs under laboratory conditions or have reported therapeutic outcomes without systematically linking device parameters to clinical efficacy. Few investigations have directly compared different LED classes under identical, clinically relevant conditions, and even fewer have quantified the impact of beam-shaping optics on achieving PBM-therapeutic irradiance at practical treatment distances. This study addresses that gap by providing a comprehensive experimental comparison of High Bright and Power LEDs, integrating electro-optical, thermal, and spectral analyses, and by demonstrating how collimating optics can enable single-emitter systems to reach therapeutic irradiance levels.

The present study aims to address this gap by experimentally characterizing and comparing the performance of commercially available red High Bright LEDs and Power LEDs in terms of their optical output, electrical characteristics, thermal behavior, and spectral properties. The effect of integrating collimating lenses on the irradiance of the Power LEDs was evaluated to determine whether PBM-relevant irradiance levels could be achieved with a single emitter. The findings provide evidence-based guidance for the design and optimization of LED-based PBM devices.

Materials and Methods

For the construction of red-light phototherapy devices, two types of high-intensity LEDs commonly available from global commercial distributors were selected and purchased: (1) High Bright LEDs and (2) Power LEDs. Both types emit red light and are specified by suppliers to have a peak emission wavelength in the range of 625–630 nm. Per typical vendor datasheets, the forward bias voltage range for the High Bright LEDs is 2.8–3.0 V, while for the Power LEDs it is 2.0–2.5 V. Power LEDs in this class are commonly offered with nominal optical/electrical ratings of 1 W and 3 W across multiple manufacturers. The Power LED purchased for use in this study had a nominal power of 1 W. For the experiments conducted in this work, ten units from each LED class were procured from commercial stock.

The output stability of the LEDs was evaluated using the setup shown in Figure 2. In this arrangement, a variable direct current (DC) power supply was employed to provide the electrical power required to operate the LEDs. A lux meter (LEYBOLD Lux-UV-IR Meter 666 243, Germany) was used to measure the illuminance of the LEDs. The lux meter had a resolution of 0.1 lx and an accuracy of ±3%. The LED and the photosensitive detector area of the lux meter were aligned along a vertical axis, facing each other. Both the LED and the lux meter were fixed in place using holders, with a separation distance of 10 cm. This distance corresponds to the working distance required for proper operation of the phototherapy device under practical treatment conditions. The measurements were performed in a controlled laboratory environment to minimize the influence of ambient light and temperature fluctuations and to facilitate reproducibility of results across laboratories. The variations in the forward current passing through the LEDs were measured simultaneously with the recording of their radiant intensity using a digital ammeter.

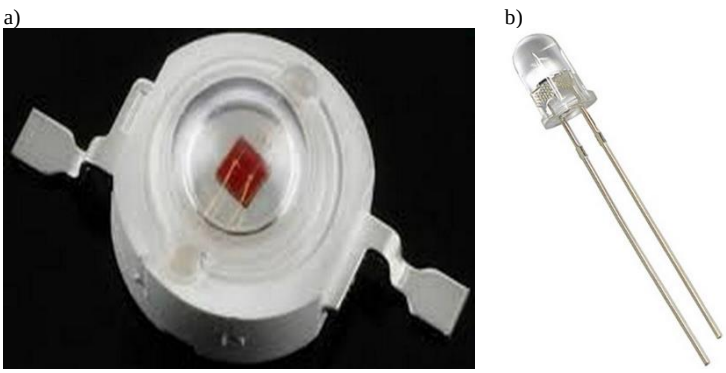

Figure 1. Two representative classes of red-emitting LEDs commonly available for high-radiance applications: (a) Power LED and (b) High Bright LED. Both classes are marketed as high-flux red emitters by multiple vendors.

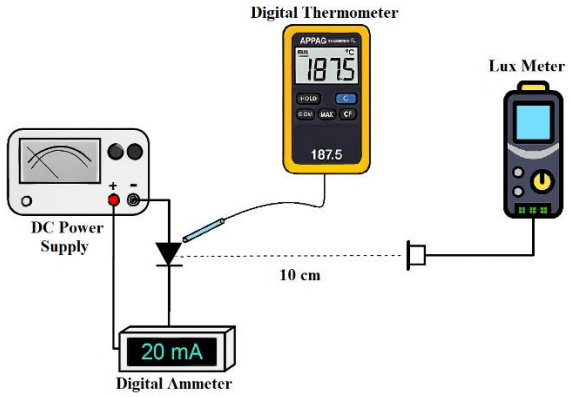

Figure 2. Schematic of the setup used for optical, electrical, and thermal characterization of LEDs.

To determine the operating voltage of the LEDs and identify the failure point, the supply voltage was increased in 0.1 V increments, while the lux meter simultaneously recorded the received light intensity. The experiment was conducted in a darkroom. A digital ammeter was connected in series with the LED circuit to record the forward current passing through the LEDs. Furthermore, the junction temperature rise generated by the LEDs was measured using a digital thermometer (APPA51) equipped with a K-type thermocouple and a 0.1 °C sensitivity. Temperature measurements were taken at the LED case surface, to ensure accurate representation of thermal behavior during operation.

The irradiance of the power LED was measured by replacing the lux meter with a calibrated photometer (Photometer, Model IL1400, FX113). The photometer was positioned at the same 10 cm distance from the LED to maintain consistency with the illuminance measurements, and readings were recorded after the LED output stabilized to avoid transient fluctuations.

The emission spectra of the LEDs were measured using a cooled electro-optic spectrometer (Thermo-Electric cooled and regulated CCD, Avantec Co., NL-6961 RB Eerbeek, Netherlands). The AvaSpect- 2048 × 14 Fiber Optic Spectrometer is a back-thinned type CCD spectrometer with high quantum efficiency and high UV sensitivity. The spectrometer was equipped with a fiber optic entrance connector (standard SMA) collimating and focusing mirror and a diffraction grating. All measurements were performed on ten independent units (n = 10) for each LED class (High Bright and Power) to ensure data reliability and reproducibility. Quantitative data are presented as the mean ± standard deviation (SD). Error bars in graphical plots represent the standard deviation across the ten tested units. Comparative analysis between LED classes was performed to assess significant differences in peak irradiance and thermal behavior.

Results

Figure 3 shows the measured radiant intensity of the LEDs as a function of supply voltage. The forward voltage threshold for the High Bright LED was determined to be approximately 2.1 ± 0.1 5 V. Increasing the voltage up to 2.4 V resulted in an almost constant radiant intensity. Beyond this voltage, the radiant intensity began to increase steadily. In the voltage range of 4.0–4.6 V, the High Bright LED approached optical output saturation, with the radiant intensity remaining nearly constant despite further voltage increases within this range. When the voltage exceeded 4.6 V, the optical performance began to decline (failure point). To prevent damage to the LED, the voltage was not increased beyond 4.9 V.

The forward voltage threshold for the Power LED was determined to be approximately 1.7 ± 0.1 V. Unlike the High Bright LED, in the Power LED, increasing the voltage beyond this threshold resulted in a gradual rise in radiant intensity without an initial plateau phase. When the voltage exceeded 2.3 V, the optical output of the Power LED began to decline (failure point). To prevent damage to the LED, the voltage was not increased beyond 2.5 V. In contrast to the High Bright LED, where the radiant intensity gradually decreased after the failure point, the Power LED exhibited a markedly more pronounced drop in radiant intensity. Another noteworthy observation was that the radiant intensities of the Power LED were substantially higher than those of the High Bright LED.

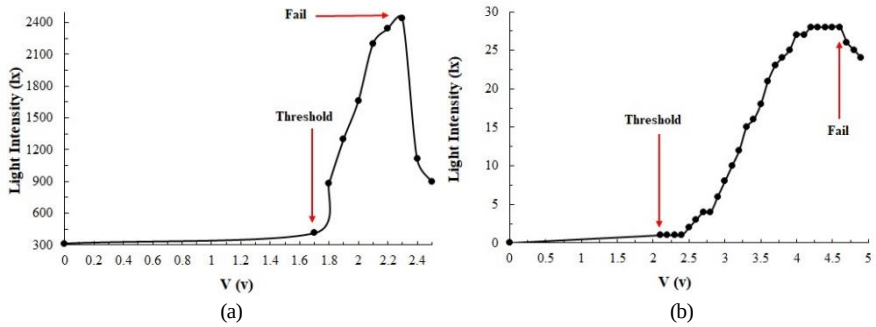

Figure 3. Optical output characteristics of the LEDs. The source–detector separation distance between the LED and the lux meter was fixed at 10 cm. (a) Power LED and (b) High Bright LED.

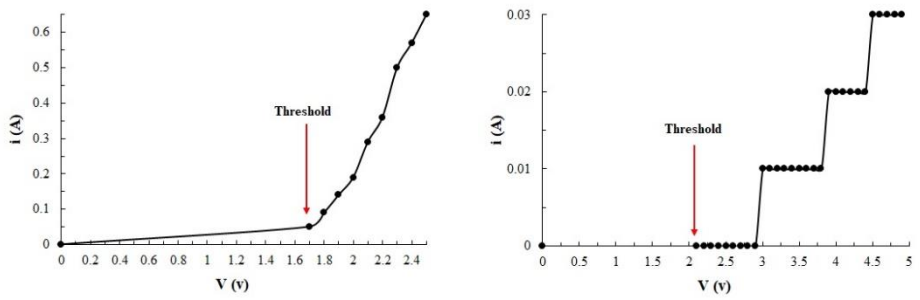

Figure 4. Forward current–voltage characteristics of the LEDs. (a) Power LED and (b) High Bright LED. The current measurement resolution of the ammeter used was approximately 0.01 A.

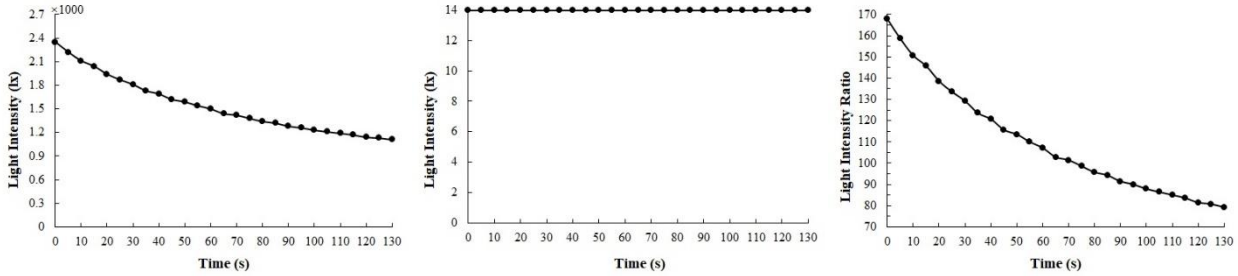

Figure 5. Comparison of the radiant intensity of the two LEDs. The source–detector separation distance between the LEDs and the lux meter was fixed at 10 cm. (a) Power LED (v_f = 2.3 V, i_f = 0.35 A) and (b) High Bright LED (v_f = 3.3 V, i_f = 0.01 A).

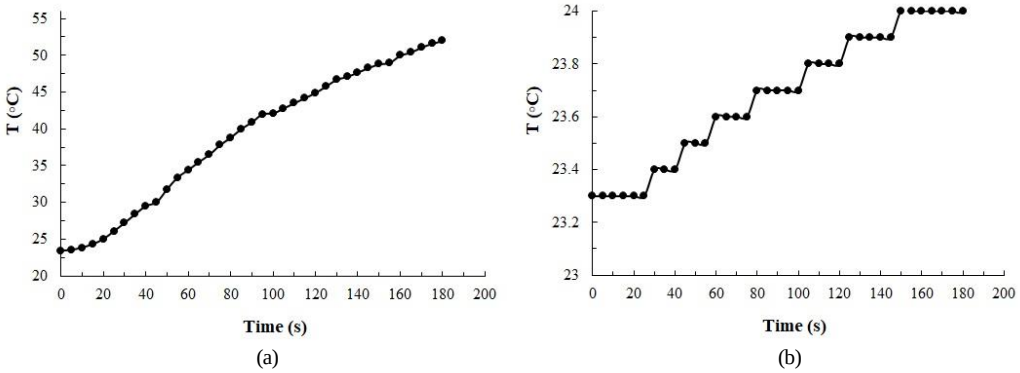

Figure 6. Comparison of the temperature rise produced by the two light sources. (a) Power LED (v_f = 2.3 V, i_f = 0.35 A) and (b) High Bright LED (v_f = 3.3 V, i_f = 0.01 A).

The forward current passing through the LEDs is presented in Figure 4. As shown in the figure, the current passing through the Power LED (Figure 4a) was considerably higher than that of the High Bright LED. Based on the obtained results, the appropriate operating voltages for long-term use were selected as 2.2 V for the Power LED and 3.3 V for the High Bright LED.

In the second experiment, the driving voltage of the LEDs was fixed at these values, and their temporal optical output stability was evaluated. Figure 5 presents the measured radiant intensity of the LEDs at a fixed source-detector distance of 10 cm over a time interval from 0 to 130 s. The radiant intensity of the High Bright LED remained constant throughout this period, whereas the radiant intensity of the Power LED decreased over time. In Figure 5c, the ratio of radiant intensities is shown to compare the two LEDs. As illustrated, the radiant intensity of the Power LED was substantially higher than that of the High Bright LED—an observation that was also readily confirmed by the unaided human eye during the experiments.

Figure 6 presents the temperature rise profiles produced by the LEDs. As shown, the temperature change produced by the High Bright LED was negligible less than 1°C after a duration of 3 minutes. In contrast, the Power LED exhibited a markedly different behavior, with a temperature increase of approximately 28.6 ± 1.2°C over the same period. To provide a quantitative perspective, the thermal resistance of the Power LED was estimated using the relation:

$$\Delta T = R_{\theta JA} \times P \quad (1)$$

where ΔT is the junction temperature rise and P is the electrical power dissipated. RθJA is the thermal resistance from junction to ambient (°C/W). At an operating point of 2.3 V and 0.35 ± 0.04 A, the input electrical power was approximately 0.8 W. With a measured case temperature increase of ~28.6°C over 180 s, the effective thermal resistance was estimated at ~35-40°C/W.

Figure 7 shows the cooling curve of the Power LED as a function of time. The time required for the LED temperature to return to ambient room temperature was approximately 4.0 ± 0.5 min.

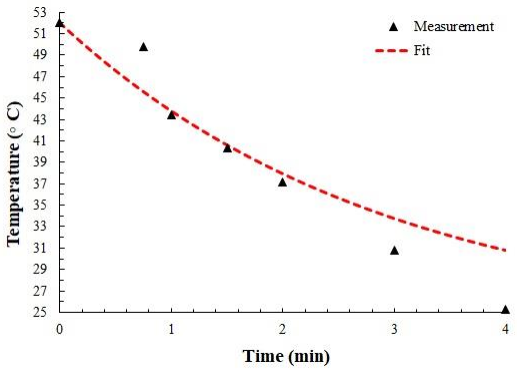

Figure 7. Cooling curve of the LED after switching off the applied 2.3 V forward bias to the power LED. A duration of approximately 4 minutes was required for the LED temperature to reach 25 °C.

Newton's Law of Cooling is a principle in heat transfer that describes how the temperature of an object changes over time when it is in a surrounding environment of a different temperature [23]:

$$T(t) = T_{env} + (T_0 - T_{env})e^{-kt} \quad (2)$$

Where T(t) is temperature of the object at time t, Tcnv is the constant ambient temperature, and k is the positive cooling constant (depends on material, surface area, airflow, etc.). After fitting, a cooling constant of k ≈ 0.3912 min-1 is obtained.

Figure 8 presents the measured emission spectra of the two types of LEDs used in this study. Table 1 lists the spectral characteristics, including the peak wavelength (630 ± 2 nm vs 636 ± 3 nm) and the FWHM (16 ± 1 nm vs 22 ± 2 nm) for each LED. Using the emission spectra, the correlated color temperature (CCT) of the LEDs was also calculated [24], and the results are provided in Table 1.

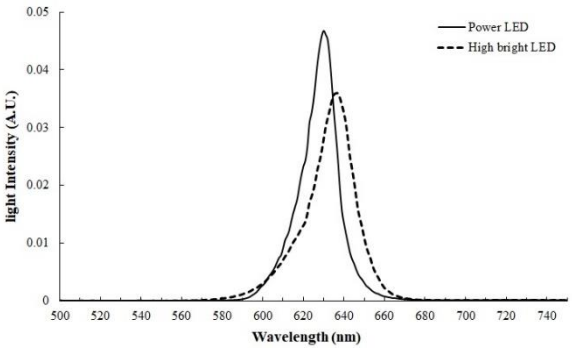

Figure 8. Measured emission spectra of the two types of LEDs in the visible spectral range.

Table 1. Emission characteristics of the LEDs

Type	CCT (Kelvin)	Peak wavelength (nm)	FWHM (nm)
Power LED	678	630	16
High bright LED	669	636	22

Figure 9 shows the changes in the irradiance of the power LED at different voltages as a function of time. The supply voltage of the power LED was adjusted to 1.8, 2.0, and 2.3 V to investigate the effect of input voltage variation on its irradiance. At 1.8 V, the irradiance remained nearly constant at approximately 250 µW/cm² throughout the 180 s measurement period. At 2.0 V, the irradiance was higher around 520 µW/cm² and also exhibited minimal variation over time. In contrast, at 2.3 V the initial irradiance was the highest, close to 720 µW/cm² but it gradually declined to about 540 µW/cm² by the end of the measurement interval.

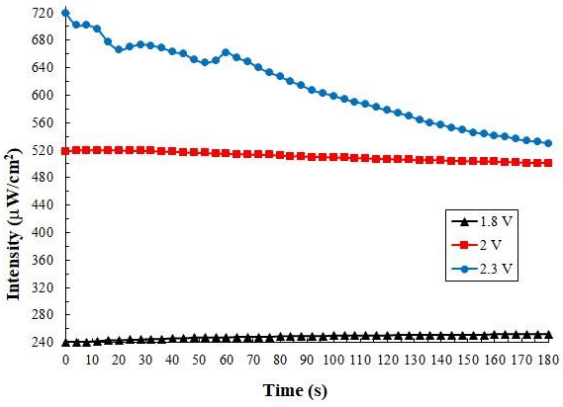

Figure 9. Variations in the irradiance of the power LED at different forward bias voltages as a function of time. The source–detector separation distance was fixed at 10 cm. When the applied voltage was reduced to 1.8 V, the LED's optical output remained nearly constant over time and, unlike at higher voltages, did not exhibit a decline. The differences in radiant exposure between the start of the experiment (t = 0 s) and the end of the experiment (t = 180 s) at voltages of 1.8, 2.0, and 2.3 V were −190, −19, and +11 µJ/cm², respectively.

Table 2. Effect of adding a collimating lens to the system on increasing the irradiance of the LED

Voltage (V)	Irradiance without lens (mW/cm²)	Irradiance with lens (mW/cm²)	Irradiance increase ratio
1.8	0.241	3.25	13.5
2	0.518	7.5	14.4
2.3	0.72	10.64	14.07

In this work, to increase the irradiance of the power LED, a 30° collimating lens was used, resulting in a half-angle beam divergence of 15°. With the lens attached to the red power LED, the irradiance at a 10 cm distance was measured at different voltages using the photometer (Table 2). Based on Table 2, it can be stated that adding a collimating lens to the LED effectively increases its irradiance. At all tested voltages, the irradiance with the lens was more than thirteen times higher than without the lens (0.72 ± 0.05 vs 10.64 ± 0.82 mW/cm² at 2.3V), with the highest relative gain (14.4x) observed at 2.0 V.

Discussion

Presenting radiant intensity versus supply voltage is a standard approach for characterizing LED electro-optical performance, as it directly links electrical drive conditions to optical output [23]. This relationship is critical for PBM applications, where precise irradiance control ensures therapeutic efficacy without exceeding safety limits. The High Bright LED threshold (2.1 V) is consistent with typical red AlGaInP LEDs, which generally exhibit forward voltages between 1.8 V and 2.2 V at room temperature [25]. Below this threshold, carrier injection is insufficient to produce significant radiative recombination, resulting in negligible light output. The rise in radiant intensity beyond 2.4 V indicates that the LED is entering a regime of higher carrier injection, where radiative recombination dominates over non-radiative processes [26]. Optical saturation in LEDs occurs when further increases in drive current no longer yield proportional increases in light output, often due to efficiency droop and thermal rollover [27]. The decline beyond this point is likely due to excessive junction heating, leading to reduced radiative efficiency and potential irreversible damage to the LED die [15]. This phenomenon, known as thermal runaway, is a critical factor in LED lifetime and reliability in phototherapy devices [1].

The absence of a plateau in the Power LED indicates that the optical output scales more directly with injected current in its normal operating range. This behavior is typical of devices designed for high-flux applications, where larger die areas and improved thermal paths allow for efficient carrier recombination over a broader current range [28]. Furthermore, for the Power LED, no saturation region similar to that observed in the High Bright LED was present. This is advantageous for applications like PBM, where maintaining high irradiance without early efficiency droop is critical. In Power LEDs, the failure point (>2.3 V) marks the onset of conditions that can accelerate degradation mechanisms such as dark line defects and phosphor thermal quenching, which are unfavorable effects for PBM devices [10].

A sharper post-failure decline in radiant intensity is characteristic of high-power LEDs when they experience rapid junction temperature rise beyond their thermal design limit [29]. The difference in radiant intensities reflects the design intent of power LEDs, which use larger chips, higher drive currents, and more efficient optical extraction to achieve higher radiant flux. For PBM applications, this higher output can be advantageous for reaching therapeutic irradiance levels at greater distances, but it also demands careful thermal management to maintain stability and avoid premature degradation [8].

This observation [of higher current] indicates the higher electrical power consumption of the Power LED compared to the High Bright LED. Higher forward current in the Power LED is expected given its design for higher luminous or radiant output. However, elevated current densities also increase junction heating, which can accelerate lumen depreciation and shorten PBM device lifetime if not adequately dissipated [30].

The stability of the High Bright LED suggests effective thermal equilibrium at its operating point, while the decline in the Power LED output is consistent with junction heating effects, where elevated temperature reduces internal quantum efficiency and increases non-radiative recombination [29]. The observed decrease in radiant intensity of the Power LED, despite a simultaneous increase in the electrical current passing through it (Figure 4a), indicates conversion losses in the form of thermal dissipation within the Power LED. The ratio of radiant intensities provides a normalized metric that highlights relative performance differences independent of absolute detector calibration, making it easier to compare LEDs under identical test conditions. For biomedical applications, higher radiant intensity must be weighed against potential thermal instability and the need for precise dosimetry [31-33].

Temperature rise profiling is a standard method for assessing the thermal performance of LEDs [34]. This stability of High Bright is consistent with the low and nearly constant forward electrical current. This substantial temperature rise of Power LED highlights the necessity of employing an appropriate thermal management mechanism when using Power LEDs in the construction of phototherapy devices. The estimated thermal resistance (~35-40°C/W) is consistent with manufacturer datasheet values for 1 W class AlGaInP LEDs (typically 30-45 °C/W). This indicates that the observed heating behavior is within expected limits, but

also underscores the importance of adequate heat sinking to prevent junction temperatures. Without adequate heat sinking, the junction temperature can quickly approach or exceed manufacturer limits, leading to reduced luminous efficacy, accelerated lumen depreciation, and shortened device lifetime.

Cooling curves are valuable for characterizing the thermal response of LEDs after power-off, as they reveal the combined effects of the device's heat dissipation pathways, and the surrounding medium's heat transfer properties [35]. The exponential form of the temperature decay is consistent with Newton's law of cooling for convective heat dissipation [36]. In LED thermal studies, this law provides a convenient way to model post-operation cooling behavior and to estimate thermal constants that reflect the device's heat dissipation efficiency [35].

Based on the results of the conducted experiments, the irradiance of the High Bright LED alone is insufficient to induce the PBM process. High Bright LEDs, while visually intense, often have lower optical power density at the treatment plane due to limited drive current capacity. Inadequate irradiance can result in sub-therapeutic fluence even if exposure time is extended, especially in tissues with higher optical attenuation [37]. Therefore, for the construction of phototherapy devices that rely on a small number of LEDs or a single LED, Power LEDs should be used. Power LEDs are designed to deliver higher radiant flux and can achieve therapeutic irradiance levels even with fewer emitters. Their higher drive currents and narrower beam angles make them more suitable for compact PBM devices [9]. However, their increased heat generation necessitates careful thermal design to maintain wavelength stability and prevent output degradation over time.

Comparing the emission spectra is critical because PBM efficacy is wavelength-dependent, with specific absorption peaks for chromophores such as cytochrome-c oxidase. The peak wavelength determines the primary tissue interaction depth, while the FWHM reflects the spectral purity of the source [6]. Narrower FWHM values can improve targeting of specific chromophores, whereas broader spectra may stimulate multiple photoacceptors but with reduced spectral efficiency [38]. In PBM, LEDs with FWHM between 20-40 nm are common, balancing chromophore specificity with manufacturing feasibility [5]. CCT can provide additional insight into spectral bias toward green or magenta, which may be relevant in multi-wavelength healthcare systems [39]. The very similar CCT values for both LEDs indicate that their overall spectral distributions produce a comparable visual color impression.

The Power LED's peak at 630 nm is known for effective PBM, where absorption by cytochrome-c oxidase is significant [4]. The High Bright LED's slightly longer peak wavelength (636 nm) may offer marginally deeper tissue penetration due to reduced scattering [6], but the difference is small and likely secondary to irradiance in determining therapeutic effect. The narrower FWHM of the Power LED (16 nm) indicates a more spectrally concentrated output, which can improve targeting of specific chromophores and reduce off-peak energy loss [40]. In PBM, narrower FWHM can be advantageous for precise wavelength targeting, while broader spectra may be beneficial in multi-target stimulation scenarios. Importantly, both LEDs tested in this study emit within the established PBM therapeutic window of 620-680 nm, where absorption by cytochrome-c oxidase and other mitochondrial chromophores is most significant.

For PBM device construction, the combination of higher radiant output and narrower FWHM makes the Power LED more suitable for applications requiring precise wavelength targeting with fewer emitters. However, its higher thermal load demands robust heat management to maintain spectral stability, as junction heating can cause peak wavelength shifts and FWHM broadening over time [41].

The minimal variation over time [at 2.0 V] suggesting that thermal effects were still limited at this operating point. The downward trend [at 2.3 V] reflects the onset of thermal rollover, where increased junction temperature reduces the LED's radiative efficiency despite constant electrical drive. The comparison across voltages clearly demonstrates that while higher drive voltages yield greater initial irradiance, they also increase susceptibility to thermal-induced output degradation over time [10].

Given that the irradiance required to initiate the PBM process is in the range of 10–50 mW/cm², the recorded values for the power LED at a 10 cm distance are not suitable for therapeutic device design. This threshold range is supported by PBM studies, which show that effective stimulation of mitochondrial chromophores such as cytochrome-c oxidase typically requires irradiances in this order of magnitude [3, 7]. The beam divergence of the LED causes irradiance to decrease with increasing distance. As the beam spreads, the same radiant flux is distributed over a larger area, reducing power density at the target plane. In PBM, this effect is particularly important because treatment distances of even a few centimeters can dramatically lower the delivered dose [2]. A simple solution to reduce LED beam divergence is to use optical lenses with collimating or beam-shaping properties. Commercially available LED lenses are classified according to the full beam after the lens. Understanding this specification is essential for predicting irradiance at a target distance and for matching optical components to therapeutic requirements. This principle allows designers to tailor beam geometry to specific clinical applications. For example, narrow-beam optics are advantageous for deep-tissue PBM where penetration is critical, while wider beams may be preferable for superficial or large-area treatments [2].

By selecting a forward bias voltage of 2.3 V for the power LED, the PBM-relevant irradiance can be reliably

achieved at a distance of 10 cm, as the measured irradiance falls within the therapeutic range of 10–50 mW/cm². These results confirm that optical beam-shaping is a highly effective method for overcoming the rapid irradiance drop caused by LED beam divergence, especially when the treatment geometry requires a fixed source-target distance [11].

From a PBM device engineering perspective, the ability to reach >10 mW/cm² at 10 cm using a single Power LED with a 30° collimating lens is significant. It means that therapeutic irradiance can be achieved without resorting to large LED arrays or excessive drive currents, both of which can increase cost, complexity, and thermal load [42]. However, the higher irradiance at 2.3 V also comes with increased thermal generation, so adequate heat sinking remains essential to maintain spectral stability and device longevity.

Conclusion

This study systematically characterized and compared the electro-optical, thermal, and spectral performance of two commercially available classes of red LEDs - High Bright and Power - under operating conditions relevant to PBM device design. The results demonstrated that, at a fixed 10 cm source–detector distance, the irradiance of the High Bright LED was insufficient to reach the PBM-therapeutic range of 10–50 mW/cm², even at its optimal operating voltage. In contrast, the Power LED delivered substantially higher radiant output and a narrower spectral bandwidth, making it more suitable for applications requiring precise wavelength targeting with fewer emitters. However, its higher drive currents and associated thermal load necessitate robust heat-management strategies to maintain output stability and spectral integrity over time.

Thermal profiling revealed negligible heating in the High Bright LED, whereas the Power LED exhibited a temperature rise of approximately 28.6 °C over three minutes, underscoring the importance of adequate heat sinking in high-power configurations. Spectral analysis confirmed that both LED types emit within the red PBM window, with the Power LED peaking at 630 nm and the High Bright LED at 636 nm. The narrower FWHM of the Power LED (16 nm) suggests greater spectral concentration and potentially improved chromophore targeting.

Beam-shaping with a 30° collimating lens increased the on-axis irradiance of the Power LED by more than thirteen-fold across all tested voltages, enabling the achievement of PBM-relevant irradiance at 10 cm with a single emitter. This approach offers a practical, cost-effective means of overcoming beam divergence without resorting to large LED arrays or excessive drive currents, though thermal considerations remain critical.

The experimental approach developed in this study is transferable to the design and optimization of therapeutic PBM devices intended for operation across a range of treatment distances and for LEDs with diverse spectral and radiometric profiles. By presenting the results in supplier-independent terms and employing optical and thermal performance metrics that are broadly applicable, the findings can be extrapolated to comparable AlGaInP-based red LEDs produced by multiple manufacturers. This generalizable framework supports reproducibility and facilitates cross-platform comparison of device performance. Future investigations should address the long-term stability of such LEDs under continuous operation, evaluate the efficacy of active thermal management strategies, and explore the integration of multi-wavelength emitter arrays to enhance therapeutic flexibility and broaden clinical applicability.

References

1. Hernández-Bule ML, Martínez-Valiente C, Serrano-Vela JI, Trillo MA. Unlocking the power of light on the skin: a comprehensive review on photobiomodulation. Int J Mol Sci. 2024;25(8):4483.
2. Zein R, Selting W, Hamblin MR. Review of light parameters and photobiomodulation efficacy: dive into complexity. J Biomed Opt. 2018;23(12):120901-120901.
3. Xu YY, Liu TCY, Cheng L. Photobiomodulation process. Int J Photoenergy. 2012;2012(1):374861.
4. Pruitt T, Choe K, Almeida-Porada G, Porada CD. Photobiomodulation at different wavelengths boosts mitochondrial redox metabolism and hemoglobin oxygenation: lasers vs. light-emitting diodes in vivo. Metabolites. 2022;12(2):103.
5. Novak J. Photobiomodulation: The Use of Specific Light Wavelengths to Accelerate Recovery, Repair, and Regeneration. In: Fundamentals of Recovery, Regeneration, and Adaptation to Exercise Stress: An Integrated Approach. Springer; 2025: 675–712.
6. Ash C, Dubec M, Donne K, Bashford T. Effect of wavelength and beam width on penetration in light-tissue interaction using computational methods. Lasers Med Sci. 2017;32(8):1909–18.
7. Kaffash Z, Hajiesmaeilbaigi F, Zandparsa R, Mozaffari H. Photobiomodulation Therapy; Survey and Principal Study Leading to Design Rules for Implants. IEEE Trans Biomed Eng. 2025.
8. Heiskanen V, Hamblin MR. Photobiomodulation: lasers vs. light emitting diodes? Photochem Photobiol Sci. 2018;17(8):1003–17.
9. Dong J, Xiong D. Applications of light emitting diodes in health care. Ann Biomed Eng. 2017;45(11):2509–23.
10. Meneghini M, Mura G, Zanoni E. Degradation mechanisms of high-power LEDs for lighting applications: An overview. IEEE Trans Ind Appl. 2013;50(1):78–85.
11. Lauret JP. Solving the optics equation for effective LED applications. Adv Opt Technol. 2012;1(1–2):65–7.
12. Syu YS, Lee YC. Quantitative evaluation of light collimating for commercial UV-LEDs based on analytic collimating lens. Appl Sci. 2022;12(2):911.
13. Chen Z, Huang S, Liu M. The review of the light parameters and mechanisms of Photobiomodulation

on melanoma cells. Photodermatol Photoimmunol Photomed. 2022;38(1):3–11.
14. Hamblin MR. Mechanisms and applications of the anti-inflammatory effects of photobiomodulation. AIMS Biophys. 2017;4(3):337.
15. Yao HW, Zhang Y, Luo H, Chen T. Failure mechanism and analysis diagnosis of LED. MAPAN. 2022;37(1):195–206.
16. Saadouni I, Abidi A, El-Bahloul S, Feki H. Optimal Thermal Management Using the Taguchi Method for LED Lighting Squared Heat Sink, Including Statistical Approaches. Sustainability. 2025;17(5):1811.
17. Su CT, Hsiao JY, Huang HC, Liou YT, Lin CH. Optimization of photobiomodulation dose in biological tissue by adjusting the focal point of lens. Photonics. 2022.
18. Yazdi ZF, Maleki A, Shokrollahi A, Karimian A. Recent progress in prompt molecular detection of liquid biopsy using Cas enzymes: innovative approaches for cancer diagnosis and analysis. J Transl Med. 2024;22(1):1173.
19. Sharif S, Ahmadi M, Ghasemi F, Esfahani H. Isolation of plasma small extracellular vesicles by an optimized size-exclusion chromatography-based method for clinical applications. J Drug Deliv Sci Technol. 2023;87:104796.
20. Aghabozorgi AS, Sadeghi MR, Nariman-Saleh-Fam Z, Hosseini R. Role of miRNA gene variants in the susceptibility and pharmacogenetics of colorectal cancer. Pharmacogenomics. 2021;22(5):303–18.
21. Khorshid Sokhangouy S, Tahmasebi S, Jalili K, Foroughi M. Recent advances in CRISPR-Cas systems for colorectal cancer research and therapeutics. Expert Rev Mol Diagn. 2024;24(8):677–702.
22. Tavakoli R, Karbalaei N, Sadeghi M, Ebrahimzadeh MH. Prolonged drug release using PCL–TMZ nanofibers induce the apoptotic behavior of U87 glioma cells. Int J Polym Mater Polym Biomater. 2018;67(15):873–8.
23. Zanhar O. Methods for Electrical and Electro-Optical Measurements on LEDs and Their Interpretation. 2025.
24. McCamy CS. Correlated color temperature as an explicit function of chromaticity coordinates. Color Res Appl. 1992;17(2):142–4.
25. Gessmann T, Schubert EF. High-efficiency AlGaInP light-emitting diodes for solid-state lighting applications. J Appl Phys. 2004;95(5):2203–16.
26. Cheng H, Zhao X, Li J, Wang S. Understanding and minimizing non-radiative recombination losses in perovskite light-emitting diodes. J Mater Chem C. 2022;10(37):13590–610.
27. Cho J, Schubert EF, Kim JK. Efficiency droop in light-emitting diodes: Challenges and countermeasures. Laser Photonics Rev. 2013;7(3):408–21.
28. Laubsch A, Sabathil M, Baur J, Lugauer H, Stutzmann M. High-power and high-efficiency InGaN-based light emitters. IEEE Trans Electron Devices. 2009;57(1):79–87.
29. Yang SC, Wu JY, Lin YF, Chen H. Failure and degradation mechanisms of high-power white light emitting diodes. Microelectron Reliab. 2010;50(7):959–64.
30. Lenk R, Lenk C. Practical lighting design with LEDs. John Wiley & Sons; 2017.
31. Beigzadeh AM, Seyed Jafari SM, Moghaddam MG, Vaziri MR. A new optical method for online monitoring of the light dose and dose profile in photodynamic therapy. Lasers Surg Med. 2020;52(7):659–70.
32. Beigzadeh AM, Vaziri MR. Z-scan dosimetry of gamma-irradiated PMMA. Nucl Instrum Methods Phys Res A. 2021;991:165022.
33. Vaziri MRR, Shakeri S, Seyfoddin E, Beigzadeh AM. Experimental investigation and simultaneous modeling of the effect of methylene blue addition to cancer tumors in photodynamic therapy by digital holography. Photodiagnosis Photodyn Ther. 2022;40:103153.
34. Poppe A, Lasance CJ. On the standardization of thermal characterization of LEDs. In: 2009 25th Annual IEEE Semiconductor Thermal Measurement and Management Symposium. IEEE; 2009.
35. Poppe A, Lasance CJ. Standardization of LED thermal characterization. In: Thermal Management for LED Applications. Springer. 2013: 197–264.
36. Maruyama S, Moriya S. Newton′s Law of Cooling: Follow up and exploration. Int J Heat Mass Transf. 2021;164:120544.
37. Algorri JF, Muñoz Ávila J, Zamarreño CR, Rodríguez-Cobo L, López-Higuera JM. Light technology for efficient and effective photodynamic therapy: a critical review. Cancers. 2021;13(14):3484.
38. Coward T, Milhazes-Cunha H, Robles AG, Purton S, Sarkis J. Utilising light-emitting diodes of specific narrow wavelengths for the optimization and co-production of multiple high-value compounds in Porphyridium purpureum. Bioresour Technol. 2016;221:607–15.
39. Wang N, Wang Y, Zhang Y, Fang J. Different light color temperatures in the morning on the effectiveness of rehabilitation training in patients with ischemic stroke: a prospective, single-center, randomized controlled clinical trial. J Neuroeng Rehabil. 2025;22(1):162.
40. Jusuf S, Dong PT. Chromophore-targeting precision antimicrobial phototherapy. Cells. 2023;12(22):2664.
41. Wu P, Ju J, Yao Q. Luminous and melanopic efficiency performance of phosphor-converted LEDs with tunable spectral characteristics. Appl Sci. 2020;10(18):6198.
42. Hadis MA, Al-Samaneh A, Ali R, Raza M, Hayes S. Development and application of LED arrays for use in phototherapy research. J Biophotonics. 2017;10(11):1514–25.